



HAL
open science

Catalytic Foldamers: When the Structure Guides the Function

Baptiste Legrand, Julie Aguesseau-Kondrotas, Matthieu Simon, Ludovic Maillard

► **To cite this version:**

Baptiste Legrand, Julie Aguesseau-Kondrotas, Matthieu Simon, Ludovic Maillard. Catalytic Foldamers: When the Structure Guides the Function. *Catalysts*, 2020, 10 (6), pp.700. 10.3390/catal10060700 . hal-04567727

HAL Id: hal-04567727

<https://hal.science/hal-04567727v1>

Submitted on 3 May 2024

HAL is a multi-disciplinary open access archive for the deposit and dissemination of scientific research documents, whether they are published or not. The documents may come from teaching and research institutions in France or abroad, or from public or private research centers.

L'archive ouverte pluridisciplinaire **HAL**, est destinée au dépôt et à la diffusion de documents scientifiques de niveau recherche, publiés ou non, émanant des établissements d'enseignement et de recherche français ou étrangers, des laboratoires publics ou privés.



Distributed under a Creative Commons Attribution 4.0 International License

Review

Catalytic Foldamers: When the Structure Guides the Function

Baptiste Legrand ¹, Julie Aguesseau-Kondrotas ¹, Matthieu Simon ² and Ludovic Maillard ^{1,*}

¹ IBMM, Université de Montpellier, CNRS, ENSCM, 34093 Montpellier, France; baptiste.legrand@umontpellier.fr (B.L.); julie.aguesseau@hotmail.fr (J.A.-K.)

² Institute of Regenerative Medicine and Biotherapies, CARTIGEN, CHU Montpellier, 34090 Montpellier, France; matthieusimon.work@gmail.com

* Correspondence: ludovic.maillard@umontpellier.fr; Tel.: +33-04-1175-9604

Received: 28 May 2020; Accepted: 18 June 2020; Published: 22 June 2020



Abstract: Enzymes are predominantly proteins able to effectively and selectively catalyze highly complex biochemical reactions in mild reaction conditions. Nevertheless, they are limited to the arsenal of reactions that have emerged during natural evolution in compliance with their intrinsic nature, three-dimensional structures and dynamics. They optimally work in physiological conditions for a limited range of reactions, and thus exhibit a low tolerance for solvent and temperature conditions. The *de novo* design of synthetic highly stable enzymes able to catalyze a broad range of chemical reactions in variable conditions is a great challenge, which requires the development of programmable and finely tunable artificial tools. Interestingly, over the last two decades, chemists developed protein secondary structure mimics to achieve some desirable features of proteins, which are able to interfere with the biological processes. Such non-natural oligomers, so called *foldamers*, can adopt highly stable and predictable architectures and have extensively demonstrated their attractiveness for widespread applications in fields from biomedical to material science. Foldamer science was more recently considered to provide original solutions to the *de novo* design of artificial enzymes. This review covers recent developments related to peptidomimetic foldamers with catalytic properties and the principles that have guided their design.

Keywords: foldamer; peptidomimetic; cooperation; organocatalyst

1. Introduction

Enzymes are incredible powerful catalysts, being typically non-toxic and environmentally friendly, while capable of performing remarkably difficult chemical transformations with relative ease, unmatched substrate, and product selectivity [1–3]. As such, they offer many opportunities in chemical industry, however, their intrinsic vulnerabilities related to their low thermal stability, low tolerance for solvent conditions, as well as their poor diversity of substrates and their high cost of production, seriously hamper their attractiveness. Besides, they display poor adaptability to abiotic chemical transformations, and the identification of suitable enzyme catalysts for a given reaction often remains a limiting step. In this context, there is a great demand for the development of enzyme mimics as proficient as their natural models but overcoming their limitations. To date, many types of enzyme mimics, ranging from polymeric [4,5] and dendritic scaffolds, supramolecular cyclodextrin and porphyrin hosts, nanoparticulates, [6–10] to catalytic antibodies [11] and natural proteins [12–14] have attempted to address some of these features.

In recent decades, great achievements have been realized following a reductionist approach in constructing catalytic sites from short artificial peptides. The discovery of short peptide sequences as effective asymmetric catalysts for a variety of reactions is now well documented and has been

extensively reviewed [15–19]. For instance, both combinatorial and *de novo* methods of catalyst design were demonstrated to successfully perform a variety of reactions including the kinetic resolutions of alcohols, aldol reactions, phosphorylation, Michael addition, and Morita–Baylis–Hillman reactions. In particular, S. Miller and H. Wennemers have emphasized the strong potential of short peptides in asymmetric catalysis [15,20]. The strength of peptide chemistry lies in the diversity and complexity that can be achieved from a small set of position-interchangeable building blocks allowing the easy access of high chemical diversity. However, the state of a short peptide in solution is generally characterized not by a single structure, but by an ensemble of conformations limiting their ability to re-create all the desirable properties for an enzyme-like catalyst.

Indeed, a fundamental paradigm in enzymology is the close relationship between the enzyme functions and their three-dimensional structures, which in turn depends on their amino acid sequences [21,22]. Large proteins of a hundred amino acids are often arranged in compact and finely tuned three-dimensional structures. The folding of polypeptide chains ensures that the residues are spatially bunched with some precision. The active sites then emerge in restricted places among the structures, constrained by the folded topology [23]. The first-shell residues at the active site are oriented in such a way as to bind the substrate and stabilize the transition state (TS) for a given reaction. The second-shell amino acids also contribute to the active site charge distribution through cooperative interactions, i.e., electrostatic, steric and hydrogen bonds. Thus, the enzymatic activity results from a necessary chemical diversity of the constituent elements; however, a tight control of the folding propensity is also just as crucial in order to encode functionally important dynamics, such as cooperative motions. Among the chemical tools reported in recent years, synthetic short oligomers, so called foldamers, [24–26] seeking to mimic the structure-forming propensity of biomolecules even at short-chain length, has provided an original contribution to this concern. Due to periodic regular H-bond networks, electronic interactions, local conformational restriction and solvophobic effects, these molecules allow the formation of programmable secondary structures, generally helices but at times strand-like conformations or turns [27,28]. In addition, while the diversity of monomer units in proteins is confined to a relatively narrow “alphabet”, determined over the course of evolution, this is not the case in foldamer chemistry where the chemical diversity is only limited by the creativity of chemists. Hence, foldamers provide an infinite range of scaffolds for presenting complex sets of functional groups to reproduce the structure and function of biomacromolecules, making them attractive for broad applications ranging from nanotechnology to biomedical fields, biopolymer surface recognition and nanomaterials. These areas are well covered in reviews [29–33]. In comparison, the catalyst function has been much more elusive for a long period. However, recent developments have led to interesting convergences between the fields of peptidomimetic foldamers and catalysis. In this review, we mainly focus on the potential of peptidomimetic foldamers including, among others, β - and γ -peptides, peptoids and oligoureas peptides for organocatalysis. We describe how a strict control of the topology could serve the design of biomimetic catalysts.

2. Principles Sustaining the Design of Catalytic Peptide Foldamers

To date, four distinct approaches have been considered in the context of organocatalysis to take advantage of the chiral microenvironment of peptidomimetic foldamers. (1) In the first one, a prosthetic group is added to the abiotic polymer. Like enzymes requiring co-factors to exert their function, for its catalytic function, the enzyme mimic depends on a group whose chemical nature is fundamentally different to the rest of the scaffold. Such a conjugation process allows for the creation of hybrid catalysts with new features resulting from the combination of the molecular recognition properties of the folded molecule with the inherent activity of the adjunct catalytic center. This strategy has been proven particularly fruitful in designing supramolecular biomacromolecules (RNA, DNA, protein) and peptide hybrids of organic and inorganic catalysts [7,9,34], but has been little explored in the field of peptidomimetic foldamers. (2) In a second approach, the peptide-like architecture is used to ensure a precise three-dimensional positioning of several key lateral side-chains that work together

in cooperation in ligand-binding and/or TS stabilization. Cooperative catalysis, defined as the dual activation of two reacting partners, is a fundamental principle of enzyme catalysis [35–38] that has guided the rational design of generations of multifunctional organocatalysts [39–42]. Cooperative enantioselective reactions can involve as either strong (mainly covalent) or transient (non-covalent) catalyst–substrate interactions [43], but whatever the mechanism, catalytic proficiency requires a very precise spatial organization of two or more reactive groups. In enzymes, the proper spatial positioning of functional groups within their active sites relies on their specific tertiary structures. In peptide foldamers, the judicious placement of the recognition elements and catalytic functional groups is simplified due the high predictability and stability of the oligomer backbone structures, and could be achieved on either a single molecule or a supramolecular assembly. (3) Besides, as demonstrated by recent studies, the well defined hydrogen-bonding network, sustaining the folding, may act by itself as support of the catalytic activity. In this third approach, the catalytic center is not shaped by the projection of reactive substitutes but directly relies on the foldamer backbone structure. In contrast to the second family of catalysts, the mechanistic characterization of catalytic asymmetric reactions involves transient, noncovalent catalyst–substrate interactions. (4) Finally, in contrast to fully artificial peptidomimetic catalysts, it has been envisioned to incorporate foldamer secondary structures into natural enzymes in order to improve and/or modify their catalytic functions. We provided an outlook on recent developments in foldamer prosthesis strategies in the last section of this review.

3. Installation of Catalytic Prosthetic Groups in Foldamers: The Peptoid Example

Kirshenbaum et al. pioneered the transfer of chiral information from a folded abiotic oligomer to an embedded prosthetic reactive center [44]. The asymmetric environment was provided by a peptoid scaffold, defined as oligomers of *N*-substituted glycine. Even though the peptoid backbone is intrinsically achiral, bulky chiral aromatic side chains such as 1-phenylethyl prompt stereocontrolled *cis*-amide helical structures resembling polyproline I [45,46]. The catalytic function was achieved by grafting (2,2,6,6-tetramethylpiperidin-1-yl)oxidanyl, commonly known as TEMPO, a competent group for oxidative transformation [47,48], at various sites along (S)-*N*-(1-phenylethyl)glycine oligomers. TEMPO is thus referred to as a redox cofactor covalently bound to helical peptoid backbones. The TEMPO–peptoid hybrids were tested for oxidative kinetic resolution of a racemic mixture of 1-phenylethanol. By modulating the position of the TEMPO group along the oligomer and by evaluating secondary structure content, the authors were able to correlate the enantioselectivity of the transformation to the helical propensity of the oligomer. In the best arrangement (Table 1, entry 3), 1 mol% of catalyst gave excellent conversion (84%) with a selectivity towards the (S) enantiomer resulting in 99% enantiomeric excess (ee) of the less reactive (*R*)-enantiomer. In contrast, when the TEMPO group was not covalently linked to the peptoid oligomer, the catalytic system 2 was still active for the oxidation of 1-phenylethanol but did not produce a transfer of the chiral information. Besides, a mixture of the 4-amino-TEMPO catalyst and (S)-1-Phenylethylamine monomer was far less effective for oxidation and did not produce enantioselective transformation (Table 1, entry 1). Collectively, these observations demonstrate a synergistic effect between the chiral environment provided by the helical peptoid scaffold, and the catalytic activity of TEMPO. The peptoid is likely to play a steric role, selectively preventing the exposure of one enantiomer to the oxidative action of the nitroxyl unit.

Table 1. Conversion, enantioselectivities and enantiomeric excess for the catalytic oxidation of 1-phenylethanol by the TEMPO–peptoid hybrids [44].

	Catalytic System	Conversion ^a (%)	Selectivity (%)	ee (%)
1		22	none	none
2		86	none	none
3		84	60 (S)	>99 (R)

(a) Conversion values are based on 2 h of reaction time.

4. Active Sites Resulting from Spatially Preorganized Reactive Side Chains

4.1. Enamine/Iminium Mediated Catalysis

Catalysis by chiral primary and secondary amines, called “aminocatalysis”, comprises two distinct reactivity manifestos for the functionalization of carbonyl compounds [49–53]. In iminium catalysis, the condensation of a nucleophile amine with a carbonyl compound generates a tetrahedral intermediate, which then converts into an iminium ion. Iminium salts are more electrophilic than the corresponding aldehydes or ketones and provide a way for electrophilic additions. When the carbonyl component is enolizable, the iminium ion is transient and evolves by deprotonation at the α -carbon atom toward a nucleophilic enamine, which can then trap electrophilic substrates (Figure 1a). Such a reversible process referred to as enamine catalysis is routinely accomplished by enzyme catalytic machinery. It has been recognized since the 1960s, that natural enzymes, such as acetoacetate decarboxylases [54,55] and type I aldolases, [56,57] use the ϵ -amino group of lysine residues for the activation of keto substrates. Compared to lysine in aqueous solution, the lysine of the Schiff base-forming enzymes has a significantly lower pKa (<7.5 versus 10.5), making them highly amenable for carbonyl condensation. Their mechanism characterization has established that the perturbation of the pKa mainly results from electrostatic interactions due to a nearby positively charged residue, often another lysine or arginine residue. This effect is further enhanced if the charged residues are almost buried in the binding pocket of the enzyme within a low dielectric environment (Figure 1b) [58,59].

These mechanistic studies have inspired Alleman and Benner for the design of lysine-rich amphiphilic α -helices as minimal oxaloacetate decarboxylase mimics [60,61]. They demonstrated a strong correlation of the catalytic activity with both the folding propensity of the peptide and the clustering of lysine side chains along one side of the helix. As in the enzyme catalytic site, placing the reacting amine close to the positively charged side chains depresses its pKa by up to two orders of magnitude due to the coulombic interactions and increases its reactivity. In 2009, Hilvert and Gellman transposed such a design onto helical β -peptides capable of forming helix bundles in aqueous media and explored their ability to catalyze the retroaldol cleavage of β -hydroxyketone [62]. β^3 -peptides typically adopt a 14-helix structure that can be further stabilized in water by the incorporation of the constrained cyclic trans-2-aminocyclohexanecarboxylic acid (ACHC) [63,64]. The resulting edifice exhibits three distinct faces enabling the perfect control of the spatial orientation of the appended functionalities.

Thus, the β -peptide sequence **11**, containing multiple ACHC residues along with β^3 -homolysine (β^3 -hLys) residues in an $i, i + 3, i + 6$ array, aligns the amine-containing side chain along one side of a 14-helix (Figure 2). Despite the absence of a true binding pocket, **11** was proficient in catalyzing with a Michaelis–Menten behavior, the retroaldol reaction of 4-phenyl-4-hydroxy-2-oxobutyrate. By adding a heptanoyl moiety at the N-terminus of the β -peptide, which promoted its self-assembly, the catalytic efficiency was enhanced by one order of magnitude. At pH 8.0 and 30 °C, the steady-state parameters k_{cat} and K_m are $0.13 \pm 0.01 \text{ min}^{-1}$ and $5.0 \pm 0.6 \text{ mM}$, respectively. The comparison of the turnover number with the rate constant for the uncatalyzed retroaldol reaction under identical conditions gives a rate acceleration of $k_{\text{cat}}/k_{\text{uncat}} = 3000$. This result highlights the benefit of clustering the β -peptides to increase both, the local positive-charge density and the hydrophobicity of the environment of catalytic amines, which in turn results in the reduction in the pKa value of the β^3 -hLys side-chain ammonium groups.

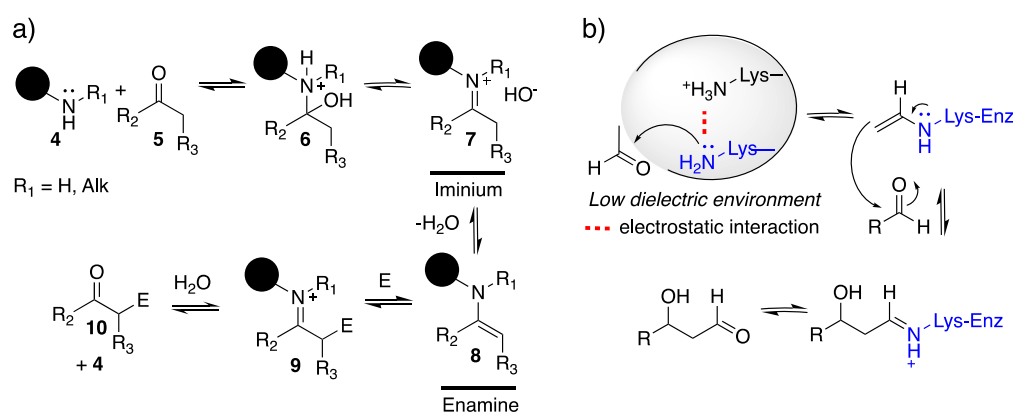


Figure 1. (a) Schematic mechanism of the enamine catalysis. E = electrophile. (b) General class I aldolase mechanism. Reactivity of the Schiff base-forming lysine is enhanced by two principal ways, a low dielectric environment and electrostatic interaction with a nearby positively charged residue.

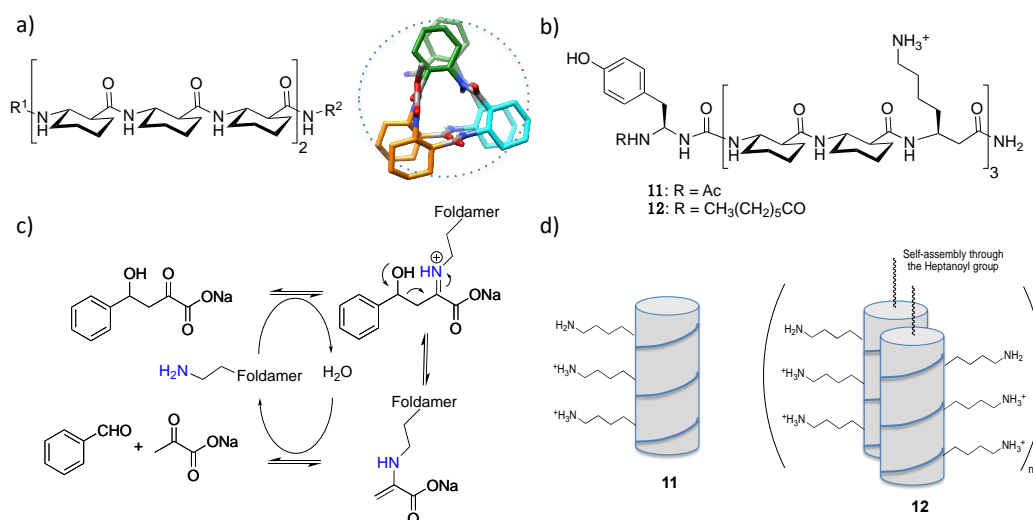


Figure 2. (a) Axis view of the helix structure of trans-2-aminocyclohexanecarboxylic acid (ACHC)-containing oligomers (CCDC: 1247870).[63] (b) Sequences of β -peptides **11**–**12**: (β^3 -hLys) residues in an $i, i + 3, i + 6$ array led to an alignment of the amine-containing side chains. (c) Retroaldol reaction of sodium 4-phenyl-4-hydroxy-2-oxobutyrate catalyzed by the β -peptides **11** and **12**. (d) Cartoon showing the 3D-organization of β -peptides **11** and **12**.

Although foldamers have huge promising potential for enamine-mediated catalysis, this research area has grown relatively slowly until the middle of the 2010s. In the 2000s, Erkkilä and Pihko reported the use of pyrrolidine as an effective catalyst for the α -methylenation reactions of aldehydes. The reaction proceeds through a second-order dependence of catalyst concentration following a Knoevenagel–Mannich-type mechanism. The catalytic cycle thus involves the dual activation of both the nucleophilic aldehyde via the enamine formation, and the electrophilic formaldehyde via the iminium formation (Figure 3a) [65]. Based on these results, Gellman's group was prompted to consider helical foldamers containing pairs of pyrrolidine-derived β -amino acid residues (so called APC) as a basis for designing a reactive dyad for the crossed aldol condensation [66]. Like its cyclopentane analogue (ACPC), APC supports the formation of a β -peptide helix characterized by $C=O(i)\cdots H-N(i+3)$ H-bonds and provides access, when it associates with L- α -amino acid residues, to diverse helical secondary structures that feature $C=O(i)\cdots H-N(i+3)$ or $C=O(i)\cdots HN(i+4)$ H-bonds. By varying the proportions of cyclic β -amino acids and L- α -amino acid residues as well as positions of the APC within the sequences, Gellman's group obtained distinct pyrrolidine diad geometries for the catalytic condensation of the α -methylenation reactions of aldehydes (Figure 3d). Among all the explored arrangements, the $\alpha/\beta/\beta$ -peptide **14** (Figure 3) led to the best catalytic efficiency with an initial rate enhancement of 143 relative to mono-APC α/β -peptide. Remarkably, structural investigations provide evidence that the $i+3$ spacing for the two APCs positions the two pyrrolidines exactly one turn apart along the helix at 5.5 ± 0.1 Å from each other. As all the other assessed geometries led to less active catalysts, such arrangement appeared to be crucial to the accommodation of a double enamine/iminium catalysis involving the two secondary amines (Figure 3). An impressive application of this concept has been a very recent achievement of the discovery of a bifunctional $\alpha/\beta/\beta$ -peptide catalyst proficient for the macrocyclization of bisaldehydes [67]. Peptide **15** acts in a dual mode, consisting of a double iminium/enamine activation of the aldehyde functions and a conformational pre-organization of the substrate so as to overcome the entropic cost of intramolecular reaction. It differs from the former hybrid peptide in that one of the catalytic units is a primary amine, which is required to activate one of the two carbonyl groups as iminium rather than enamine. The efficient foldamer-catalyzed macrocyclization was demonstrated to be practical for the synthesis of large-ring natural products, e.g., nostocycline A.

In recent years, our group explored a class of constrained heterocyclic γ -amino acids built around a thiazole ring, so called ATCs (4-amino(methyl)-1,3-thiazole-5-carboxylic acids). Thanks to the planar conformation of the $\gamma C-\beta C-\alpha C-C(O)$ torsion angle imposed by the heterocycles, ATC oligomers adopt a nine-helix structure resulting from the formation of a highly stable C_9 hydrogen-bonding pattern [68,69]. These foldamers could be readily functionalized [70] and the helical structure showed a low dependency on the appended side chains. Among other applications [71,72], we were interested in addressing ATC molecules for enamine-type catalysis [73]. We first established the effectiveness of a dual ATC monomer catalyst **16** on the nitro-Michael addition reaction of cyclohexanone and β -*trans*-nitrostyrene (Figure 4). With a nucleophilic pyrrolidine in position 2 of the thiazole core and a propanoic chain on the γ carbon lateral chain, ATC **16** could be viewed as a structural analog of the H–D–Pro–Pro–Glu–NH₂ tripeptide, which is probably the most efficient catalyst for such a transformation [74–77].

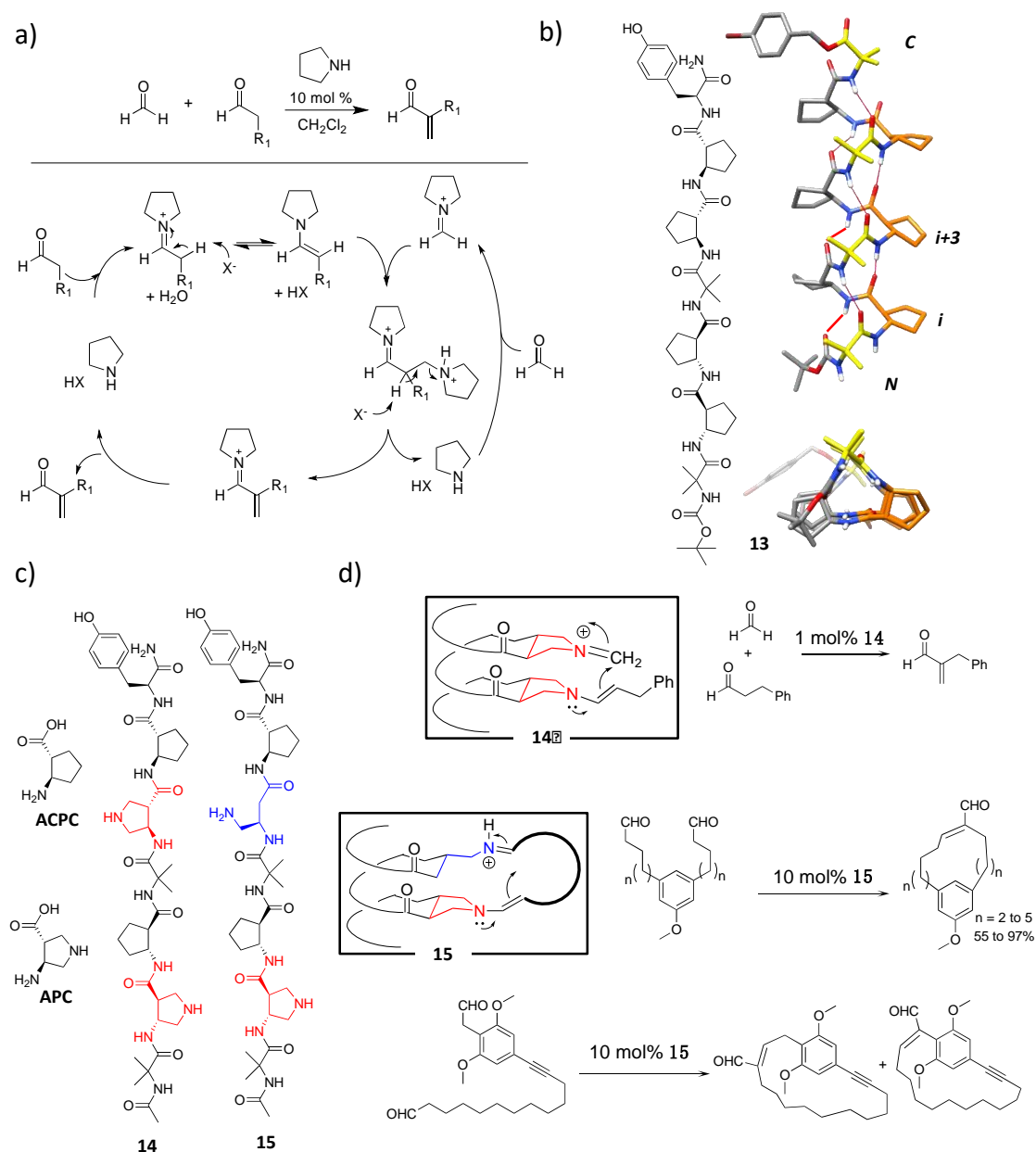


Figure 3. (a) Mechanism of the pyrrolidine-catalyzed α -methylation of aldehydes [65]. (b,c) α/β -peptide bifunctional catalysts **14** and **15** were designed based on the helical secondary structures adopted by the ACPC-containing foldamer **13** (CSD: PUCDEX). (d) Foldamer-catalyzed α -methylation and macrocyclization (reaction conditions: 2 equiv. triethylamine, 2 equiv. propionic acid, 4 vol % water, *i*-PrOH, 37 °C).

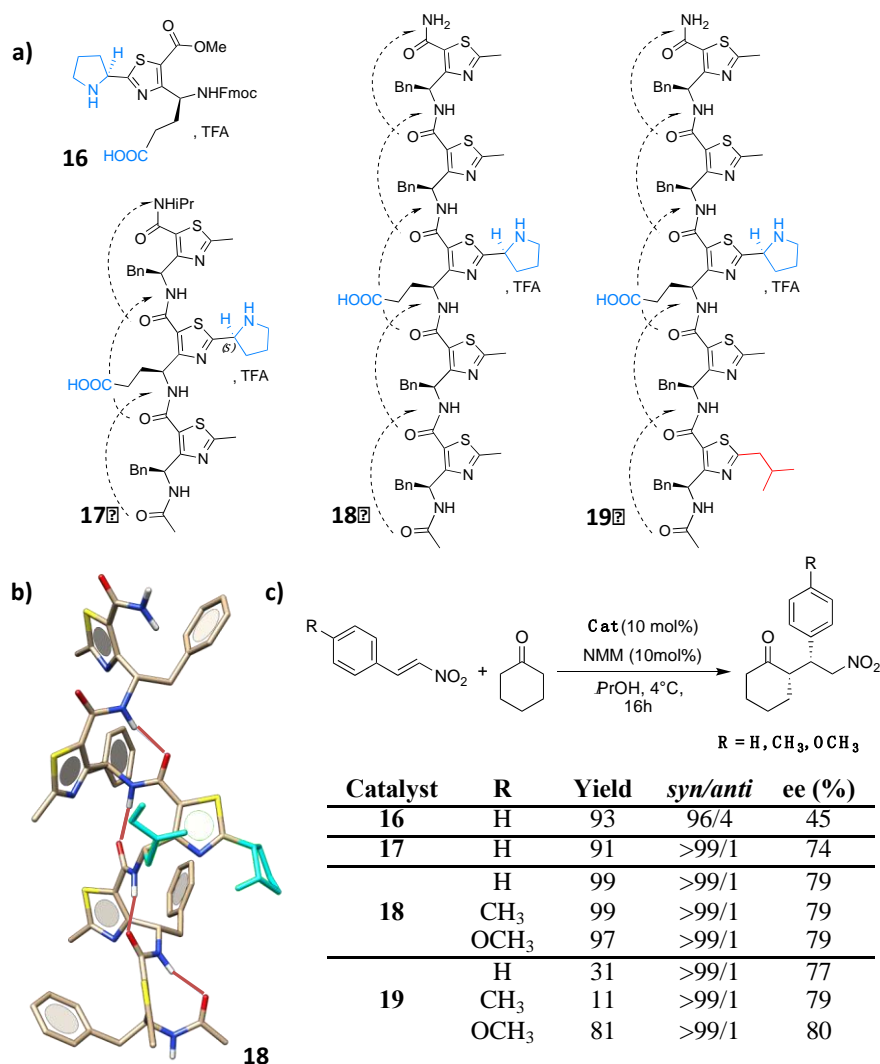


Figure 4. (a) ATC (4-amino(methyl)-1,3-thiazole-5-carboxylic acids)-based catalysts. (b) Lowest energy NMR solution structures of **18** in *i*PrOH. Catalytic groups are in light blue. (c) Nitro-Michael addition reaction of cyclohexanone to β -trans-nitrostyrene (R=H), trans-4-methyl- (R=CH₃) and trans-4-methoxy- β -nitrostyrene (R=OCH₃) using ATC-based catalysts.

Compound **16** showed a high catalytic activity toward the *syn* isomer, up to 45% ee for the (*S*, *R*) enantiomer. Including the catalytic residue in a folded γ -peptide (peptides **17** and **18**, Figure 4) enhanced the asymmetric induction (*syn/anti* = 96:4; ee = 79%), highlighting that the nine-helix structure is likely to contribute to the enantioselectivity [73]. Structure/activity studies revealed that side chains distant from the catalytic residue had a somewhat surprisingly effect on substrate selectivity. For instance, sequence **19** with a branched lateral chain at the N-terminus showed a marked preference for *trans*-4-methoxy- β -nitrostyrene while it was poorly active for the transformation of β -*trans*-nitrostyrene, and *trans*-4-methyl- β -nitrostyrene. Such a feature, reminiscent of biological catalysts, is not really understood but underlines the effect of a complex environment in orienting substrate selectivity.

4.2. Bundle Foldamers as Artificial Esterase

Engineering entirely new enzymes from scratch still remains an inaccessible challenge owing in part to the difficulty in predicting the atomic level conformation of a polypeptide sequence. However, over the last decade, seminal works on coiled-coil proteins [78–81] have opened up the prospect of

designing globular protein-like helix-bundle quaternary structures based on β^3 -peptide [82–85] and oligoureia foldamers [86–88]. Among the reported structures, the group of A. Schepartz described the most thermally and kinetically stable β^3 -peptide bundle characterized to date [89]. The octameric bundle assembly (Figure 5a) named Zwit-EYYK **20** consists of parallel and antiparallel 14-helices, well packed by a leucine-rich core and arrays of salt-bridge interactions involving β^3 -homoornithines. In 2014, Zwit-EYYK was considered as a starting point for the rational design of an esterase mimic using 8-acetoxypyrene-1,3,6-trisulfonate **23** as a model substrate [90]. In the first step, the peptide sequence was modified to create binding sites for the anionic substrate. This was achieved by mutating the two β^3 -homoornithine residues sharing one face of the helix (positions 3 and 9) by two β^3 -homoarginines known to interact favorably with sulfonate groups. Secondly, the hydrolytic activity was installed by adding a basic histidine residue at the N-terminus of the peptide. Considering that each bundle comprises four parallel, two antiparallel, and four tetramer–tetramer helical contacts, and there are two active sites per interhelical interface, there are theoretically 20 intermolecular active sites per bundle.

The resulting foldamer **21** was able to catalyze the hydrolysis of **23** in a Michaelis–Menten behavior with a turnover 588-times faster than the uncatalyzed reaction ($k_{\text{cat}}/K_m = 54 \text{ M}^{-1} \text{ min}^{-1}$). However, the bundle self-assembly was impaired at the concentration chosen for the steady-state kinetics studies (25 mM) but was restored by covalently joining two monomers via a tetra- β -homoglycine linker (compound **22**, Figure 5c). At low concentration of substrate (<200 μM), the catalytic efficiency was improved by nearly two orders of magnitude ($k_{\text{cat}}/K_m = 5102 \text{ M}^{-1} \text{ min}^{-1}$), compared to the monomeric species **21**. The enhancement of the reaction showed to be related to an increase in affinity for the substrate ($K_m = 4$ and 345 μM for **22** and **21** respectively), which can be explained by the greater number of functional esterolytic active sites within the supramolecular architecture relative to the single chain catalyst. However, at high concentration of substrate, the kinetic failed to follow the Michaelis–Menten model and the hydrolytic rate decreased toward an asymptote. This unexpected behavior was interpreted as a substrate inhibition phenomenon, which is commonly observed as a regulatory mechanism of natural enzymes. The origin of the inhibition is actually not understood but revealed nonproductive catalyst–substrate interactions.

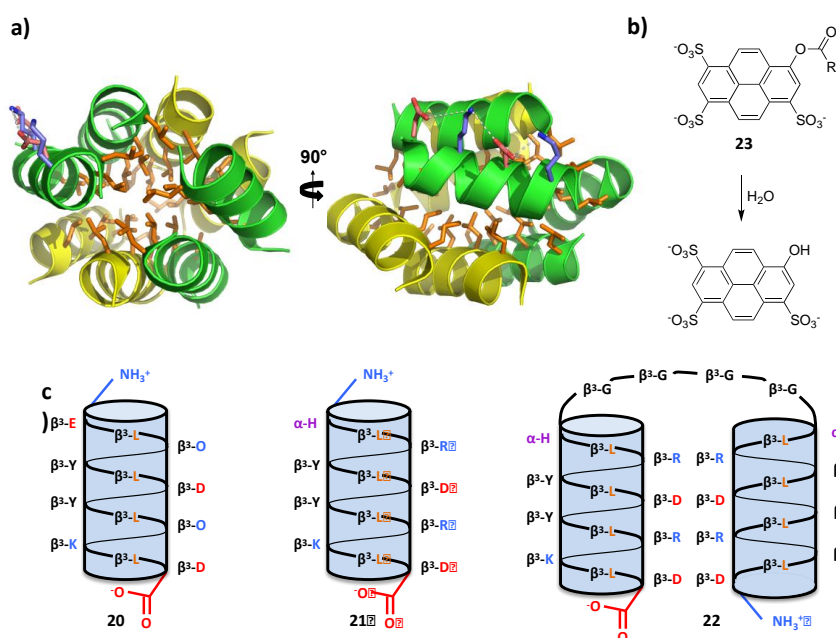


Figure 5. (a) Structure of the octameric Zwit-EYYK bundle (CCDC 804 687). Key residues for the bundle stabilization are depicted as follows: orange: β^3 -hLeu; blue: β^3 -hOrn; and red: β^3 -hAsp. (b) Hydrolysis of 8-acetoxypyrene-1,3,6-trisulfonate **23**, chosen as a model reaction. (c) Helical net diagrams of Zwit-EYYK **20** and esterolytic-active β^3 -peptides **21–22**.

5. Hydrogen-Bond Catalysis Directed by the Main Chain Atoms

A deeper understanding of the enzyme-catalyzed processes has extensively highlighted the crucial role of hydrogen bonding as both a structural and catalytic determinant of enzyme active sites. For instance, the stabilization of negatively charged oxygens in transition states often takes place via two, or sometimes even three, hydrogen bonds directed at the substrate oxygen atom [91,92]. This is referred to as an oxyanion hole-based mechanism. Generally, the oxyanion holes pre-exist in the unliganded enzymes, thus considerably lowering the entropic cost of redirecting the H-bond donors in the active site. From these observations, the concept of hydrogen-bonding catalysis has been formulated. This review will not attempt to exhaustively examine the extensive literature on hydrogen-bond catalysis and the interested reader is invited to read selected reviews [93–95]. The aim here is to explore how short folded oligomers can be used as control elements for directing H-bond catalysis. The first work in this field dates back to 40 years ago, with the publication of the asymmetric poly-L-leucine (PLL)-catalyzed nucleophilic epoxidation of electron deficient olefins, such as α , β -unsaturated ketones (Figure 6a). The reaction referred to as the Julia–Colonna epoxidation consists of a bi- or triphasic system comprising the insoluble PLL peptide, H_2O_2 as an oxidant, and a base in a water-immiscible solvent [96–98]. Extensive kinetic explorations demonstrated that the PLL behaves as an enzyme-like catalyst with a first-order dependence on both the hydroperoxide anion ($K_M = 30$ mM) and the enone substrate ($K_M = 110$ mM) [99,100]. Oxidation takes place through a steady-state random bireactant mechanism, which implicates that all substrates must bind to the catalyst to generate a tertiary complex (PLL– HOO^- –enone). The rapid equilibrium enabling the complex formation is followed by the rate-limiting formation of the peroxide enolate. However, for a long time, the precise location of the catalytic site remained elusive. Structural investigations provided evidence for the α -helix propensity of PLL. Interestingly, only five amino acids, which correspond to one helical turn, are sufficient to catalyze the epoxidation reaction [101]. In α -helix, the four N-terminal N–H groups of the polypeptide chain are not engaged in intra-chain hydrogen bonds (Figure 6b), and subsequently, are available as acceptors for hydrogen bonding with the enone and the peroxide enolate. In addition, the resulting oxyanion hole benefits from the cooperative charge stabilization by the α -helix macrodipole [102]. Molecular mechanics calculations confirmed the binding mode of a chalcone peroxyenolate to NH-2, NH-3 and NH-4 (Figure 6b). This structural framework proved to be general. Other folded polyamino acids [100] and helical β^3 -peptides [103] also catalyzed the epoxidation of chalcones. Despite the different structural features from α -peptides, poly- β^3 -leucines are able to catalyze the epoxidation of (*E*)- α , β -enones with enantioselectivity up to 85%. The exact mechanism by which β^3 -peptides interplays with the substrates to transfer the chiral information is not described. It is likely that similarly to PLL, the main-chain atoms are involved in the catalysis. However, the orientation of the N–H bonds within the typical β^3 -peptidic helices is opposite to those of α -helices, which excludes the binding site at the N-terminus and makes the C-terminus extremity a possible active site.

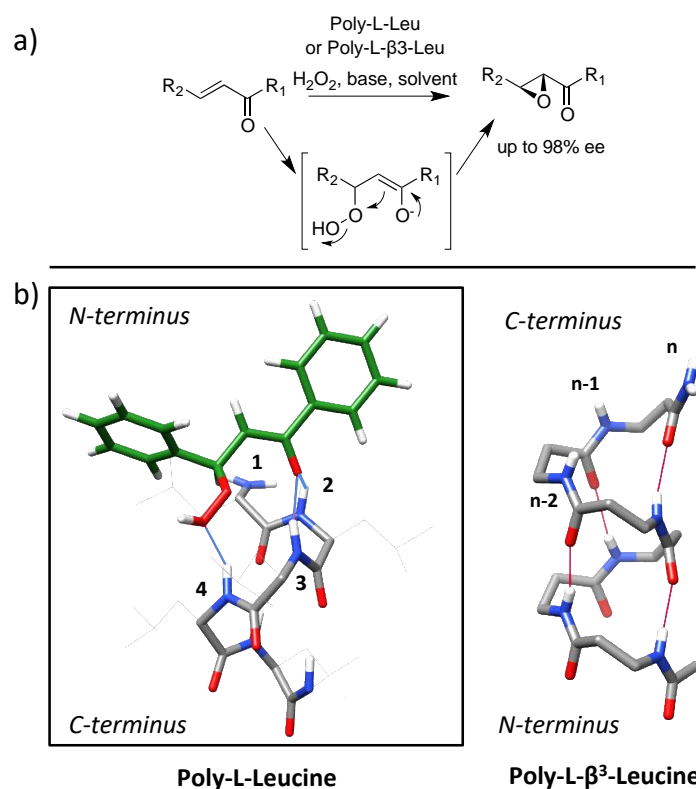


Figure 6. (a) Scheme of the poly-L-leucines and poly-L- β^3 -peptides-catalyzed oxidation of α,β -unsaturated ketones by hydrogen peroxide under basic conditions. The reaction proceeds through a resonance-stabilized peroxide enolate intermediate. (b) Left: model for the binding of the chalcone peroxyenolate to the NH-2, NH-3 and NH-4 of PLL (forest green chalcone enolate hydroperoxide; built using UCSF Chimera according to [100]). Right: the proposed binding site of poly-L- β^3 -peptides involves the amide protons n , $n-1$ and $n-2$ at the C-terminus extremity.

The intrinsic reactivity of helical peptides has long been confined to chalcone epoxidation, but in recent years, there has been renewed interest in this field with the discovery of new reaction possibilities. This includes the work of Tanaka et al. who described helical peptide-catalyzed enantioselective Michael addition reactions [104,105]. As in the Julia–Colonna epoxidation, mechanistic considerations supported the participation of the *N*-terminal amide protons in the activation of the nucleophile species through H-bonding coordination. Very recently, Guichard et al. extended the concept of backbone-mediated catalysis to aliphatic *N,N'*-linked oligoureas [106]. Over the last decade, this group established the propensity of these oligomers to fold into a 2.5-type helix promoted by a network of three-centered hydrogen bonds between $C=O(i)$ and urea $HN(i-3)$ and $HN'(i-2)$ [107–109]. Since the first two ureas at the positive end of the oligourea helix macrodipole do not participate in intra-chain hydrogen bonding (Figure 7a), it has been proposed that they may provide an ideal set of acceptors to create an oxyanion hole. Their efficiency in binding anions confirmed this hypothesis, paving the way for developments of oligoureas in the field of catalysis (Figure 7b) [110]. Among H-bond donor groups acting as oxyanion hole mimics, (thio) ureas have shown to be highly effective, promoting carbon–carbon and carbon–heteroatom bond formation, either as monofunctional catalyst with the assistance of an external base or as an integral part of a bifunctional Brønsted base-H-bond catalyst [111–114]. Helical oligo (thio) urea foldamers have thus naturally been considered for the catalysis of enantioselective carbon–carbon bond formation reactions. Foldamer **23a**, in association with an external Brønsted base, was extraordinarily effective in the enantioselective conjugate addition reaction of malonate esters and nitroalkenes even at a charge of catalyst as low as 0.01 mol% (Figure 7a). As in PLL, [101,102] the reactivity of the hydrogen bond donor sites is enhanced by the cooperative charge stabilization provided by the directional hydrogen bond network spreading along the foldamer (Figure 7c).[102,115,116]

Hexamer **23b**, which contains a thiourea in the first position, also performed well but was systematically less effective than **23a** in the addition of malonate to the nitroolefine. This result is unintuitive but one plausible explanation given by the authors is that the benefit of increasing the acidity by replacing the oxygen of the first urea by a sulfur atom is counterbalanced by unfavorable conformational change and dynamics at the positive pole of the helix where catalysis takes place.

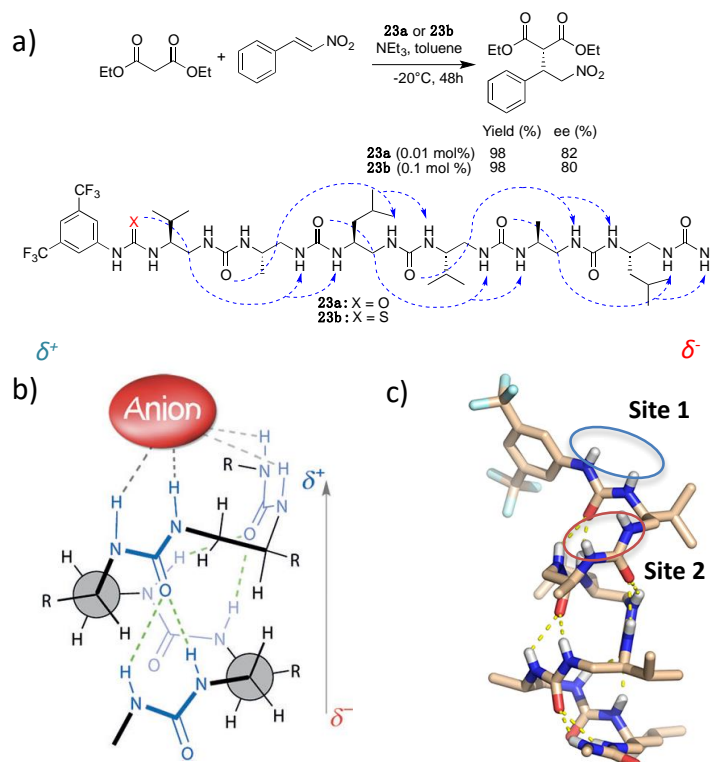


Figure 7. (a) Conjugate addition of diethylmalonate to nitroalkenes catalyzed by *N,N'*-linked oligoureas **23a–b**. The H-bond network (dashed curve) evidences the disponibility of the two ureas at the positive end of the oligourea. (b) Model for the binding of anion to *N,N'*-linked oligoureas [110]. (c) X-ray crystal structure of **23a** showing the accessibility of H-bond donor sites (Picture from [106]).

In the former example, the chirality of the transformation is intimately guided by the asymmetric folding of the oligomer, which depends on the stereochemistry of the monomer units. The inversion of enantioselectivity requires the switching of all the stereochemical centers, making the synthesis tedious. An interesting approach to overcome this concern is to use an achiral oligomer and induce symmetry breaking by an external stimulus. This concept was explored by Clayden et al. on Aib oligomers as support of the catalysis. Aib oligomers are intrinsically achiral and they mainly populate two 3_{10} -helical conformations in opposite screw senses. However, adding a chiral residue in either the N- or C terminal position or even by using chiral groups that bind the helix in a non-covalent manner lead to an imbalance in the population of the two interconverting screw-sense conformers [117–120]. This ability was used to control the stereochemical environment of a bifunctional achiral aminothiourea moiety placed at the N-terminus of the oligomer [121]. The remotely inducible chiral thiourea center was proficient in the catalysis of the enantioselective nitro-Michael addition reaction of diethylmalonate to β -trans-nitrostyrene. Adding a photoswitchable AlaBni residue at the C-terminus of the oligomer made the photo-induced inversion of the helix screw-sense possible, which in turn changed the enantioselectivity of the reaction (Figure 8).

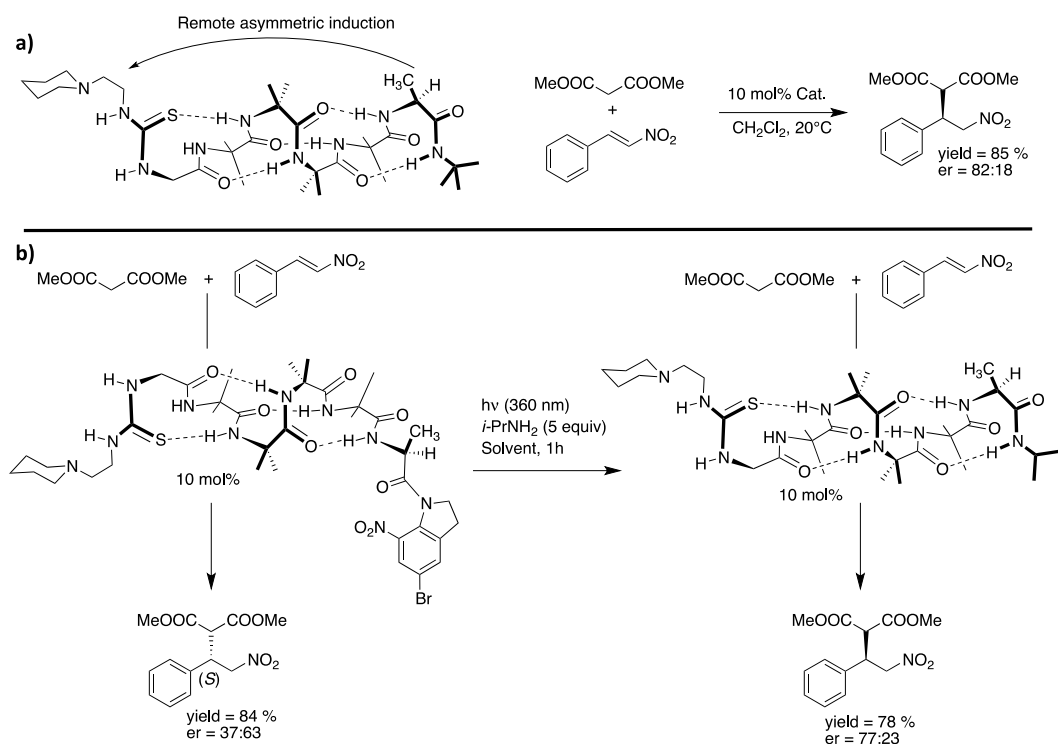


Figure 8. (a) Catalytic oligourea with a remotely inducible chiral catalytic site for the nitro-Michael addition reaction of diethylmalonate to β-trans-nitrostyrene. (b) Photochemical refolding of a catalytic foldamer with the consequent inversion of the sense of asymmetric induction [121].

6. Foldamers as Protein Prosthesis

The whole foldamers presented in the above sections were designed through bottom-up approaches. The edifices were able to catalyze a specific transformation, taking advantage of the topological control of the oligomer scaffolds. However, compared to natural enzymes, they lacked well defined binding pockets, thus limiting their proficiency and selectivity. The group of A. Schepartz attempted to remedy this issue through foldamer bundle assemblies [90]. As a result, the protein-like particle displayed multiple active sites differing in their local microenvironments and catalytic aptitudes. In recent years, consideration was given to the substitution of whole secondary structure elements of a protein with topographical mimics, whilst retaining the function of the parent protein [122–124]. Such an approach has been termed “protein-prosthesis” or “bionic proteins” and has been recently investigated in designing foldamer-enzyme hybrids with true binding pockets [125,126].

In a seminal example, S. Gellman and D. Hilvert developed a functional heterodimeric chorismate mutase (CM) through the non-covalent association of a α/β-peptide foldamer with an inactive three-helix domain of the enzyme. In the native protein from *Methanococcus jannaschii*, the CM catalytic site is formed at the interface of a four α-helix bundle (Figure 9a). It was previously showed that cleaving the dimer-spanning N-terminal helix to yield a one-helix and a three-helix fragment abolishes enzyme function. However, attaching a leucine zipper dimerization domain to the two polypeptides results in the spontaneous assembly of the two fragments, returning a split enzyme with wild-type-like activities [127]. This property was used as a starting point to develop foldamer-hybrid variants of the split CM, in which the one-helix domain was substituted by α/β-peptide surrogates differing in the number, location and/or type of β³-residues. Attaching a leucine-zipper dimerization domain to the foldamers ensured their association with the triple helix fragment (Figure 9b). While the α/β-peptides alone were unable to catalyze the conversion of chorismate, enzyme-like activities were observed with the hybrid assemblies. A similar demonstration of the functional plasticity of proteins to the introduction of artificial segments has been recently described by Wilson starting from a split version

of RNase S as protein scaffold [126]. An α -helix segment of the catalytic site, bearing one of the two histidine residues required for acid-base catalyzed hydrolysis of the phosphodiester linkage in RNA, was successfully replaced by an aromatic oligoamide foldamer [126]. The proteomimetics were shown to display first-order kinetics with enzymatic efficiency dependent on both the concentration of proteomimetic and RNA, but, with an efficiency $>10^4$ -fold lower than for the fully functional RNase S-protein/S-peptide complex.

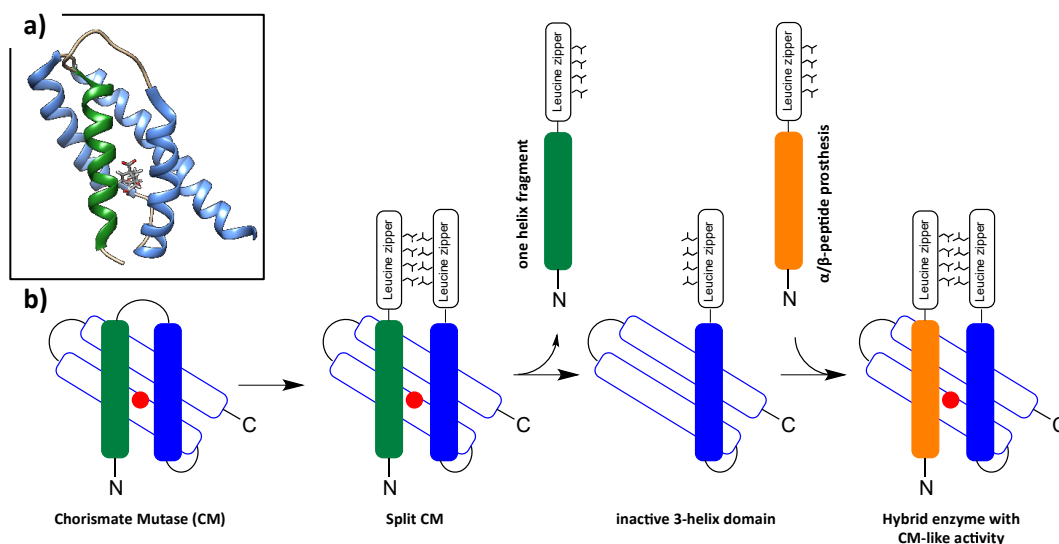


Figure 9. (a) Ribbon diagrams of the monomeric chorismate mutase (PDB code 2gtv) [128]. (b) Schematic representation of chorismate mutase (CM) and its split variant. Exchange of the one helix fragment (green) with a α/β -peptide surrogate (orange) led to a hybrid enzyme with CM-like activity. The active site is symbolized by a red circle [121].

7. Conclusions

Foldamers can mimic the structural and biological properties of biopolymers and interesting applications were developed in various fields from life to material science. They were more recently considered as valuable scaffolds as catalysts able to mimic complex reactions as natural enzymes. These latter are quite sophisticated and finely tuned machines and the *de novo* design of artificial enzymes remains highly challenging. Fortunately, we showed herein that the use of peptidomimetic foldamers is particularly relevant to address this challenge since they putatively exhibit an infinite range of structures and a huge chemical diversity. The high stability and the predictability of the foldamer architectures allow to accurately position and maintain chemical functions at ideal distances, while their overall fold can confine the substrate into a reactive conformation, thus overcoming the entropic cost of intramolecular reactions mimicking the enzyme active sites. If such aptitudes are actually out of reach with small molecule catalysts, the development of real binding pockets using foldamers to re-create the natural enzymes microenvironments remains a major obstacle to override the enzymes' performances while operating in various conditions (including temperature, solvent and concentration). Moreover, the cooperativity is probably the central paradigm for future achievements in the design of proficient catalytic foldamers. Nevertheless, research in this field has just begun and chemists are far from exhausting the potential of peptidomimetic foldamers in catalysis.

Funding: This research received no external funding.

Conflicts of Interest: The authors declare no conflict of interest.

References

1. Nestl, B.M.; Hammer, S.C.; Nebel, B.A.; Hauer, B. New generation of biocatalysts for organic synthesis. *Angew. Chem. Int. Ed. Engl.* **2014**, *53*, 3070–3095. [[CrossRef](#)] [[PubMed](#)]
2. Voet, D.; Voet, J.G. *Biochemistry*, 3rd ed.; Publisher: New York, NY, USA, 2004.
3. Schomburg, I.; Chang, A.; Placzek, S.; Sohngen, C.; Rother, M.; Lang, M.; Munaretto, C.; Ulas, S.; Stelzer, M.; Grote, A.; et al. BRENDA in 2013: Integrated reactions, kinetic data, enzyme function data, improved disease classification: New options and contents in BRENDA. *Nucleic Acids Res.* **2013**, *41*, D764–D772. [[CrossRef](#)]
4. Wulff, G. Enzyme-like catalysis by molecularly imprinted polymers. *Chem. Rev.* **2002**, *102*, 1–27. [[CrossRef](#)] [[PubMed](#)]
5. Suh, J.S. Synthesis of polymeric enzyme-like catalysts. *Synlett* **2001**, *9*, 1343–1363. [[CrossRef](#)]
6. Kirby, A.J. Enzyme mechanisms, models, and mimics. *Angew. Chem. Int. Ed. Engl.* **1996**, *35*, 707–724. [[CrossRef](#)]
7. Raynal, M.; Ballester, P.; Vidal-Ferran, A.; van Leeuwen, P.W. Supramolecular catalysis. Part 2: Artificial enzyme mimics. *Chem. Soc. Rev.* **2014**, *43*, 1734–1787. [[CrossRef](#)]
8. Kuah, E.; Toh, S.; Yee, J.; Ma, Q.; Gao, Z. Enzyme mimics: Advances and applications. *Chem. Eur. J.* **2016**, *22*, 8404–8430. [[CrossRef](#)]
9. Yin, Y.; Dong, Z.; Luo, Q.; Liu, J. Biomimetic catalysts designed on macromolecular scaffolds. *Prog. Polym. Sci.* **2012**, *37*, 1476–1509. [[CrossRef](#)]
10. Song, W.; Zhao, B.; Wang, C.; Ozaki, Y.; Lu, X. Functional nanomaterials with unique enzyme-like characteristics for sensing applications. *J. Mater. Chem. B* **2019**, *7*, 850–875. [[CrossRef](#)]
11. Stevenson, J.D.; Thomas, N.R. Catalytic antibodies and other biomimetic catalysts. *Nat. Prod. Rep.* **2000**, *17*, 535–577. [[CrossRef](#)]
12. Qi, D.; Tann, C.M.; Haring, D.; Distefano, M.D. Generation of new enzymes via covalent modification of existing proteins. *Chem. Rev.* **2001**, *101*, 3081–3111. [[CrossRef](#)] [[PubMed](#)]
13. Ostermeier, M. Engineering allosteric protein switches by domain insertion. *Protein Eng. Des. Sel.* **2005**, *18*, 359–364. [[CrossRef](#)] [[PubMed](#)]
14. Creus, M.; Ward, T.R. Designed evolution of artificial metalloenzymes: protein catalysts made to order. *Org. Biomol. Chem.* **2007**, 1835–1844. [[CrossRef](#)] [[PubMed](#)]
15. Davie, E.A.; Mennen, S.M.; Xu, Y.; Miller, S.J. Asymmetric catalysis mediated by synthetic peptides. *Chem. Rev.* **2007**, *107*, 5759–5812. [[CrossRef](#)]
16. Miller, S.J. In search of peptide-based catalysts for asymmetric organic synthesis. *Acc. Chem. Res.* **2004**, *37*, 601–610. [[CrossRef](#)]
17. Mogharabi, M.; Rezaei, S.; Faramarzi, M.A. Peptide-catalysis in asymmetric organic synthesis. *Trends Pept. Protein Sci.* **2017**, *1*, 89–98. [[CrossRef](#)]
18. Zozulia, O.; Dolan, M.A.; Korendovych, I.V. Catalytic peptide assemblies. *Chem. Soc. Rev.* **2018**, *47*, 3621–3639. [[CrossRef](#)]
19. Akagawa, K. *Peptide Applications in Biomedicine, Biotechnology and Bioengineering*; Elsevier Inc.: Amsterdam, The Netherlands, 2018; pp. 513–564. [[CrossRef](#)]
20. Wennemers, H. Asymmetric catalysis with peptides. *Chem. Commun.* **2011**, *47*, 12036–12041. [[CrossRef](#)]
21. Redfern, O.C.; Dessailly, B.; Orengo, C.A. Exploring the structure and function paradigm. *Curr. Opin. Struct. Biol.* **2008**, *18*, 394–402. [[CrossRef](#)]
22. Dessailly, B.H.; Redfern, O.C.; Cuff, A.; Orengo, C.A. Exploiting structural classifications for function prediction: Towards a domain grammar for protein function. *Curr. Opin. Struct. Biol.* **2009**, *19*, 349–356. [[CrossRef](#)]
23. Freiburger, M.I.; Guzovsky, A.B.; Wolynes, P.G.; Parra, R.G.; Ferreira, D.U. Local frustration around enzyme active sites. *Proc. Natl. Acad. Sci. USA* **2019**, *116*, 4037–4043. [[CrossRef](#)] [[PubMed](#)]
24. Hill, D.J.; Mio, M.J.; Prince, R.B.; Hughes, T.S.; Moore, J.S. A field guide to foldamers. *Chem. Rev.* **2001**, *101*, 3893–4012. [[CrossRef](#)] [[PubMed](#)]
25. Guichard, G.; Huc, I. Synthetic foldamers. *Chem. Commun.* **2011**, *47*, 5933–5941. [[CrossRef](#)] [[PubMed](#)]
26. Hecht, S.; Huc, I. *Foldamers: Structure, Properties And Applications*; Wiley-VCH Verlag GmbH & Co.: Weinheim, Germany, 2007; p. 425. [[CrossRef](#)]

27. Roy, A.; Prabhakaran, P.; Baruah, P.K.; Sanjayan, G.J. Diversifying the structural architecture of synthetic oligomers: The hetero foldamer approach. *Chem. Commun.* **2011**, *47*, 11593–11611. [[CrossRef](#)]
28. Martinek, T.A.; Fulop, F. Peptidic foldamers: Ramping up diversity. *Chem. Soc. Rev.* **2012**, *41*, 687–702. [[CrossRef](#)] [[PubMed](#)]
29. Goodman, C.M.; Choi, S.; Shandler, S.; DeGrado, W.F. Foldamers as versatile frameworks for the design and evolution of function. *Nat. Chem. Biol.* **2007**, *3*, 252–262. [[CrossRef](#)] [[PubMed](#)]
30. Baptiste, B.; Godde, F.; Huc, I. How can folded biopolymers and synthetic foldamers recognize each other. *Chembiochem* **2009**, *10*, 1765–1767. [[CrossRef](#)] [[PubMed](#)]
31. Gopalakrishnan, R.; Frolov, A.I.; Knerr, L.; Drury, W.J., III; Valeur, E. Therapeutic potential of foldamers: From chemical biology tools to drug candidates. *J. Med. Chem.* **2016**, *59*, 9599–9621. [[CrossRef](#)]
32. Checco, J.W.; Gellman, S.H. Targeting recognition surfaces on natural proteins with peptidic foldamers. *Curr. Opin. Struct. Biol.* **2016**, *39*, 96–105. [[CrossRef](#)]
33. Kulkarni, K.; Habila, N.; Del Borgo, M.P.; Aguilar, M.I. Novel materials from the supramolecular self-assembly of short helical beta(3)-peptide foldamers. *Front. Chem.* **2019**, *7*, 70. [[CrossRef](#)]
34. Wang, T.; Fan, X.; Hou, C.; Liu, J. Design of artificial enzymes by supramolecular strategies. *Curr. Opin. Struct. Biol.* **2018**, *51*, 19–27. [[CrossRef](#)] [[PubMed](#)]
35. Dugas, H. *Bioorganic Chemistry A Chemical Approach to Enzyme Action, Chapter 4*; Springer: New York, NY, USA, 1996; pp. 159–251.
36. Silverman, R.B. *Organic Chemistry of Enzyme-Catalyzed Reactions, Chapter 1*; Academic Press: San Diego, CA, USA, 2002. [[CrossRef](#)]
37. Hedstrom, L. Serine protease mechanism and specificity. *Chem. Rev.* **2002**, *102*, 4501–4524. [[CrossRef](#)]
38. Cleland, W.W.; Hengge, A.C. Enzymatic mechanisms of phosphate and sulfate transfer. *Chem. Rev.* **2006**, *106*, 3252–3278. [[CrossRef](#)] [[PubMed](#)]
39. Breslow, R. Bifunctional acid-base catalysis by imidazole groups in enzyme mimics. *J. Mol. Cat.* **1994**, *91*, 161–174. [[CrossRef](#)]
40. Peters, R.E.A. *Cooperative Catalysis Designing Efficient Catalysts for Synthesis*; Wiley-VCH Verlag GmbH & Co.: Weinheim, Germany, 2015; p. 456.
41. Wende, R.C.; Schreiner, P.R. Evolution of asymmetric organocatalysis: Multi- and retrocatalysis. *Green Chem.* **2012**, *14*, 1821–1849. [[CrossRef](#)]
42. Zhou, J. *Multi-Catalyst System in Asymmetric Catalysis*; Wiley: Hoboken, NJ, USA, 2014; p. 1.
43. Liu, F. The upside of downsizing: Asymmetric trifunctional organocatalysts as small enzyme mimics for cooperative enhancement of both rate and enantioselectivity with regulation. *Chirality* **2013**, *25*, 675–683. [[CrossRef](#)]
44. Maayan, G.; Ward, M.D.; Kirshenbaum, K. Folded biomimetic oligomers for enantioselective catalysis. *Proc. Natl. Acad. Sci. USA* **2009**, *106*, 13679–13684. [[CrossRef](#)]
45. Kirshenbaum, K.; Barron, A.E.; Goldsmith, R.A.; Armand, P.; Bradley, E.K.; Truong, K.T.; Dill, K.A.; Cohen, F.E.; Zuckermann, R.N. Sequence-specific polypeptoids: A diverse family of heteropolymers with stable secondary structure. *Proc. Natl. Acad. Sci. USA* **1998**, *95*, 4303–4308. [[CrossRef](#)]
46. Wu, C.W.; Sanborn, T.J.; Huang, K.; Zuckermann, R.N.; Barron, A.E. Peptoid oligomers with alpha-chiral, aromatic side chains: Sequence requirements for the formation of stable peptoid helices. *J. Am. Chem. Soc.* **2001**, *123*, 6778–6784. [[CrossRef](#)]
47. Anelli, P.L.; Biffi, C.; Montanari, F.; Quici, S. Fast and selective oxidation of primary alcohols to aldehydes or to carboxylic acids and of secondary alcohols to ketones mediated by oxoammonium salts under two-phase conditions. *J. Org. Chem.* **1987**, *52*, 2559–2562. [[CrossRef](#)]
48. Anelli, P.L.; Banfi, S.; Montanari, F.; Quici, S. Oxidation of diols with alkali hypochlorites catalyzed by oxammonium salts under two-phase conditions. *J. Org. Chem.* **1989**, *54*, 2970–2972. [[CrossRef](#)]
49. List, B. Enamine catalysis is a powerful strategy for the catalytic generation and use of carbanion equivalents. *Acc. Chem. Res.* **2004**, *37*, 548–557. [[CrossRef](#)] [[PubMed](#)]
50. Mukherjee, S.; Yang, J.W.; Hoffmann, S.; List, B. Asymmetric enamine catalysis. *Chem. Rev.* **2007**, *107*, 5471–5569. [[CrossRef](#)]
51. Pihko, P.M.; Majander, I.; Erkkilä, A. Enamine Catalysis. In *Asymmetric Organocatalysis. Topics in Current Chemistry*; List, B., Ed.; Springer: Berlin/Heidelberg, Germany, 2010; Volume 291.

52. Giacalone, F.; Gruttadauria, M.; Agrigento, P.; Noto, R. Low-loading asymmetric organocatalysis. *Chem. Soc. Rev.* **2012**, *41*, 2406–2447. [[CrossRef](#)] [[PubMed](#)]
53. Notz, W.; Tanaka, F.; Barbas, C.F., III. Enamine-based organocatalysis with proline and diamines: The development of direct catalytic asymmetric Aldol, Mannich, Michael, and Diels-alder reactions. *Acc. Chem. Res.* **2004**, *37*, 580–591. [[CrossRef](#)]
54. Hamilton, G.A.; Westheimer, F.H. On the mechanism of the enzymatic decarboxylation of acetoacetate. *J. Am. Chem. Soc.* **1959**, *81*, 6332–6333. [[CrossRef](#)]
55. Laursen, R.A.; Westheimer, F.H. The active site of acetoacetate decarboxylase. *J. Am. Chem. Soc.* **1966**, *88*, 3426–3430. [[CrossRef](#)]
56. Grazi, E.; Rowley, P.T.; Cheng, T.; Tchola, O.; Horecker, B.L. The mechanism of action of aldolases. III. Schiff base formation with lysine. *Biochem. Biophys. Res. Commun.* **1962**, *9*, 38–43. [[CrossRef](#)]
57. Lai, C.Y.; Nakai, N.; Chang, D. Amino acid sequence of rabbit muscle aldolase and the structure of the active center. *Science* **1974**, *183*, 1204–1206. [[CrossRef](#)]
58. Westheimer, F.H. Coincidences, decarboxylation, and electrostatic effects. *Tetrahedron* **1995**, *51*, 3–20. [[CrossRef](#)]
59. Heine, A.; Luz, J.G.; Wong, C.H.; Wilson, I.A. Analysis of the class I aldolase binding site architecture based on the crystal structure of 2-deoxyribose-5-phosphate aldolase at 0.99Å resolution. *J. Mol. Biol.* **2004**, *343*, 1019–1034. [[CrossRef](#)] [[PubMed](#)]
60. Johansson, K.; Allemann, R.K.; Widmer, H.; Benner, S.A. Synthesis, structure and activity of artificial, rationally designed catalytic polypeptides. *Nature* **1993**, *365*, 530–532. [[CrossRef](#)] [[PubMed](#)]
61. Weston, C.J.; Cureton, C.H.; Calvert, M.J.; Smart, O.S.; Allemann, R.K. A stable miniature protein with oxaloacetate decarboxylase activity. *ChemBioChem* **2004**, *5*, 1075–1080. [[CrossRef](#)] [[PubMed](#)]
62. Muller, M.M.; Windsor, M.A.; Pomerantz, W.C.; Gellman, S.H.; Hilvert, D. A rationally designed aldolase foldamer. *Angew. Chem. Int. Ed. Engl.* **2009**, *48*, 922–925. [[CrossRef](#)]
63. Appella, D.H.; Christianson, L.A.; Klein, D.A.; Powell, D.R.; Huang, X.; Barchi, J.J., Jr.; Gellman, S.H. Residue-based control of helix shape in beta-peptide oligomers. *Nature* **1997**, *387*, 381–384. [[CrossRef](#)]
64. Raguse, T.L.; Lai, J.R.; Gellman, S.H. Environment-independent 14-helix formation in short beta-peptides: Striking a balance between shape control and functional diversity. *J. Am. Chem. Soc.* **2003**, *125*, 5592–5593. [[CrossRef](#)]
65. Erkkilä, A.; Pihko, P.M. Rapid organocatalytic aldehyde-aldehyde condensation reactions. *Eur. J. Org. Chem.* **2007**, 4205–4216. [[CrossRef](#)]
66. Girvin, Z.C.; Gellman, S.H. Exploration of diverse reactive diad geometries for bifunctional catalysis via foldamer backbone variation. *J. Am. Chem. Soc.* **2018**, *140*, 12476–12483. [[CrossRef](#)]
67. Girvin, Z.C.; Andrews, M.K.; Liu, X.; Gellman, S.H. Foldamer-templated catalysis of macrocycle formation. *Science* **2019**, *366*, 1528–1531. [[CrossRef](#)]
68. Mathieu, L.; Legrand, B.; Deng, C.; Vezenkov, L.; Wenger, E.; Didierjean, C.; Amblard, M.; Averlant-Petit, M.C.; Masurier, N.; Lisowski, V.; et al. Helical oligomers of thiazole-based gamma-amino acids: Synthesis and structural studies. *Angew. Chem. Int. Ed. Engl.* **2013**, *52*, 6006–6010. [[CrossRef](#)]
69. Bonnel, C.; Legrand, B.; Bantignies, J.L.; Petitjean, H.; Martinez, J.; Masurier, N.; Maillard, L.T. FT-IR and NMR structural markers for thiazole-based gamma-peptide foldamers. *Org. Biomol. Chem.* **2016**, *14*, 8664–8669. [[CrossRef](#)]
70. Mathieu, L.; Bonnel, C.; Masurier, N.; Maillard, L.T.; Martinez, J.; Lisowski, V. Cross-Claisen condensation of n-fmoc-amino acids—A short route to heterocyclic γ -amino acids. *Eur. J. Org. Chem.* **2015**, *2015*, 2262–2270. [[CrossRef](#)]
71. Ali, L.M.A.; Simon, M.; El Cheikh, K.; Aguesseau-Kondrotas, J.; Godefroy, A.; Nguyen, C.; Garcia, M.; Morere, A.; Gary-Bobo, M.; Maillard, L. Topological requirements for CI-M6PR-Mediated cell uptake. *Bioconjug. Chem.* **2019**, *30*, 2533–2538. [[CrossRef](#)]
72. Simon, M.; Ali, L.M.A.; Cheikh, K.E.; Aguesseau, J.; Gary-Bobo, M.; Garcia, M.; Morère, A.; Maillard, L.T. Can heterocyclic γ -peptides provide polyfunctional platforms for synthetic glycocluster construction. *Chem. Eur. J.* **2018**, *24*, 11426–11432. [[CrossRef](#)] [[PubMed](#)]

73. Aguesseau-Kondrotas, J.; Simon, M.; Legrand, B.; Bantignies, J.L.; Kang, Y.K.; Dumitrescu, D.; Van Der Lee, A.; Campagne, J.M.; de Figueiredo, R.M.; Maillard, L.T. Prospect of Thiazole-based gamma-peptide foldamers in enamine catalysis: Exploration of the Nitro-michael addition. *Chem. Eur. J.* **2019**, *25*, 7396–7401. [[CrossRef](#)] [[PubMed](#)]
74. Wiesner, M.; Revell, J.D.; Tonazzi, S.; Wennemers, H. Peptide catalyzed asymmetric conjugate addition reactions of aldehydes to nitroethylene—A convenient entry into gamma2-amino acids. *J. Am. Chem. Soc.* **2008**, *130*, 5610–5611. [[CrossRef](#)] [[PubMed](#)]
75. Wiesner, M.; Revell, J.D.; Wennemers, H. Tripeptides as efficient asymmetric catalysts for 1,4-addition reactions of aldehydes to nitroolefins—A rational approach. *Angew. Chem. Int. Ed. Engl.* **2008**, *47*, 1871–1874. [[CrossRef](#)]
76. Wiesner, M.; Neuburger, M.; Wennemers, H. Tripeptides of the type H-D-Pro-Pro-Xaa-NH₂ as catalysts for asymmetric 1,4-addition reactions: Structural requirements for high catalytic efficiency. *Chem. Eur. J.* **2009**, *15*, 10103–10109. [[CrossRef](#)]
77. Wiesner, M.; Upert, G.; Angelici, G.; Wennemers, H. Enamine catalysis with low catalyst loadings—high efficiency via kinetic studies. *J. Am. Chem. Soc.* **2010**, *132*, 6–7. [[CrossRef](#)]
78. Moffet, D.A.; Hecht, M.H. De novo proteins from combinatorial libraries. *Chem. Rev.* **2001**, *101*, 3191–3203. [[CrossRef](#)]
79. Hecht, M.H.; Das, A.; Go, A.; Bradley, L.H.; Wei, Y. De novo proteins from designed combinatorial libraries. *Protein Sci.* **2004**, *13*, 1711–1723. [[CrossRef](#)] [[PubMed](#)]
80. Burkhard, P.; Stetefeld, J.; Strelkov, S.V. Coiled coils: A highly versatile protein folding motif. *Trends Cell Biol.* **2001**, *11*, 82–88. [[CrossRef](#)]
81. Woolfson, D.N. The design of coiled-coil structures and assemblies. *Adv. Protein Chem.* **2005**, *70*, 79–112. [[CrossRef](#)] [[PubMed](#)]
82. Giuliano, M.W.; Horne, W.S.; Gellman, S.H. An alpha/beta-peptide helix bundle with a pure beta3-amino acid core and a distinctive quaternary structure. *J. Am. Chem. Soc.* **2009**, *131*, 9860–9861. [[CrossRef](#)]
83. Horne, W.S.; Price, J.L.; Gellman, S.H. Interplay among side chain sequence, backbone composition, and residue rigidification in polypeptide folding and assembly. *Proc. Natl. Acad. Sci. USA* **2008**, *105*, 9151–9156. [[CrossRef](#)]
84. Daniels, D.S.; Petersson, E.J.; Qiu, J.X.; Schepartz, A. High-resolution structure of a beta-peptide bundle. *J. Am. Chem. Soc.* **2007**, *129*, 1532–1533. [[CrossRef](#)]
85. Wang, P.S.; Schepartz, A. Beta-peptide bundles: Design. Build. Analyze. Biosynthesize. *Chem. Commun.* **2016**, *52*, 7420–7432. [[CrossRef](#)]
86. Collie, G.W.; Bailly, R.; Pulka-Ziach, K.; Lombardo, C.M.; Mauran, L.; Taib-Maamar, N.; Dessolin, J.; Mackereth, C.D.; Guichard, G. Molecular recognition within the cavity of a foldamer helix bundle: Encapsulation of primary alcohols in aqueous conditions. *J. Am. Chem. Soc.* **2017**, *139*, 6128–6137. [[CrossRef](#)]
87. Lombardo, C.M.; Collie, G.W.; Pulka-Ziach, K.; Rosu, F.; Gabelica, V.; Mackereth, C.D.; Guichard, G. Anatomy of an oligoureic six-helix bundle. *J. Am. Chem. Soc.* **2016**, *138*, 10522–10530. [[CrossRef](#)]
88. Collie, G.W.; Pulka-Ziach, K.; Lombardo, C.M.; Fremaux, J.; Rosu, F.; Decossas, M.; Mauran, L.; Lambert, O.; Gabelica, V.; Mackereth, C.D.; et al. Shaping quaternary assemblies of water-soluble non-peptide helical foldamers by sequence manipulation. *Nat. Chem.* **2015**, *7*, 871–878. [[CrossRef](#)]
89. Craig, C.J.; Goodman, J.L.; Schepartz, A. Enhancing beta3-peptide bundle stability by design. *ChemBioChem* **2011**, *12*, 1035–1038. [[CrossRef](#)] [[PubMed](#)]
90. Wang, P.S.; Nguyen, J.B.; Schepartz, A. Design and high-resolution structure of a beta(3)-peptide bundle catalyst. *J. Am. Chem. Soc.* **2014**, *136*, 6810–6813. [[CrossRef](#)] [[PubMed](#)]
91. Pihko, P.M.; Rapakko, S.; Wierenga, R.K. *Hydrogen Bonding in Organic Synthesis*; Wiley-VCH Verlag GmbH: Mörlenbach, Germany, 2009.
92. Kamerlin, S.C.; Chu, Z.T.; Warshel, A. On catalytic preorganization in oxyanion holes: Highlighting the problems with the gas-phase modeling of oxyanion holes and illustrating the need for complete enzyme models. *J. Org. Chem.* **2010**, *75*, 6391–6401. [[CrossRef](#)] [[PubMed](#)]
93. Schreiner, P.R. Metal-free organocatalysis through explicit hydrogen bonding interactions. *Chem. Soc. Rev.* **2003**, *32*, 289–296. [[CrossRef](#)] [[PubMed](#)]

94. Taylor, M.S.; Jacobsen, E.N. Asymmetric catalysis by chiral hydrogen-bond donors. *Angew. Chem. Int. Ed. Engl.* **2006**, *45*, 1520–1543. [[CrossRef](#)]
95. Zhang, Z.; Schreiner, P.R. (Thio)Urea organocatalysis—What can be learnt from anion recognition. *Chem. Soc. Rev.* **2009**, *38*, 1187–1198. [[CrossRef](#)]
96. Juliá, S.; Masana, J.; Vega, J.C. “Synthetic enzymes”. Highly stereoselective epoxidation of chalcone in a triphasic toluene-water-poly[(S)-alanine] system. *Angew. Chem. Int. Ed. Engl.* **1980**, *19*, 929–931.
97. Juliá, S.; Guixer, J.; Masana, J.; Rocas, J.; Colonna, S.; Annuziata, R.; Molinari, H. Synthetic enzymes. Part 2. Catalytic asymmetric epoxidation by means of polyamino-acids in a triphase system. *J. Chem. Soc. Perkin Trans.* **1982**, *1*, 1317–1324. [[CrossRef](#)]
98. Allen, J.V.; Drauz, K.H.; Flood, R.W.; Roberts, S.M.; Skidmore, J. Polyamino acid-catalysed asymmetric epoxidation: Sodium percarbonate as a source of base and oxidant. *Tet. Lett.* **1999**, *40*, 5417–5420. [[CrossRef](#)]
99. Carrea, G.; Colonna, S.; Meek, A.D.; Ottolina, G.; Roberts, S.M. Kinetics of chalcone oxidation by peroxide anion catalysed by poly-l-leucine. *Chem. Commun.* **2004**, 1412–1413. [[CrossRef](#)]
100. Carrea, G.; Colonna, S.; Kelly, D.R.; Lazcano, A.; Ottolina, G.; Roberts, S.M. Polyamino acids as synthetic enzymes: Mechanism, applications and relevance to prebiotic catalysis. *Trends Biotechnol.* **2005**, *23*, 507–513. [[CrossRef](#)]
101. Berkessel, A.; Gasch, N.; Glaubitz, K.; Koch, C. Highly enantioselective enone epoxidation catalyzed by short solidphase-bound peptides: Dominant role of peptide helicity. *Org. Lett.* **2001**, *3*, 3839–3842. [[CrossRef](#)] [[PubMed](#)]
102. Kelly, D.R.; Roberts, S.M. The mechanism of polyleucine catalysed asymmetric epoxidation. *Chem. Commun.* **2004**, 2018–2020. [[CrossRef](#)]
103. Coffey, P.E.; Drauz, K.H.; Roberts, S.M.; Skidmore, J.; Smith, J.A. beta-peptides as catalysts: Poly-beta-leucine as a catalyst for the Julia-Colonna asymmetric epoxidation of enones. *Chem. Commun.* **2001**, 2330–2331. [[CrossRef](#)]
104. Ueda, A.; Umeno, T.; Doi, M.; Akagawa, K.; Kudo, K.; Tanaka, M. Helical-peptide-catalyzed enantioselective michael addition reactions and their mechanistic insights. *J. Org. Chem.* **2016**, *81*, 6343–6356. [[CrossRef](#)]
105. Umeno, T.; Ueda, A.; Doi, M.; Kato, T.; Oba, M.; Tanaka, M. Helical foldamer-catalyzed enantioselective 1,4-addition reaction of dialkyl malonates to cyclic enones. *Tet. Lett.* **2019**, *60*, 151301. [[CrossRef](#)]
106. Becart, D.; Diemer, V.; Salaun, A.; Oiarbide, M.; Nelli, Y.R.; Kauffmann, B.; Fischer, L.; Palomo, C.; Guichard, G. Helical oligourea foldamers as powerful hydrogen bonding catalysts for enantioselective C-C bond-forming reactions. *J. Am. Chem. Soc.* **2017**, *139*, 12524–12532. [[CrossRef](#)] [[PubMed](#)]
107. Burgess, K.; Ibarzo, J.; Linthicum, D.S.; Russell, D.H.; Shin, H.; Shitangkoon, A.; Totani, R.; Zhang, A.J. Solid phase syntheses of oligoureas. *J. Am. Chem. Soc.* **1997**, *119*, 1556–1564. [[CrossRef](#)]
108. Semetey, V.; Rognan, D.; Hemmerlin, C.; Graff, R.; Briand, J.-P.; Marraud, M.; Guichard, G. Stable helical secondary structure in short-chain N,N'-linked oligoureas bearing proteinogenic side chains. *Angew. Chem. Int. Ed. Engl.* **2002**, *41*, 1893–1895. [[CrossRef](#)]
109. Fischer, L.; Claudon, P.; Pendem, N.; Miclet, E.; Didierjean, C.; Ennifar, E.; Guichard, G. The canonical helix of urea oligomers at atomic resolution: Insights into folding-induced axial organization. *Angew. Chem. Int. Ed. Engl.* **2010**, *122*, 1085–1088. [[CrossRef](#)]
110. Diemer, V.; Fischer, L.; Kauffmann, B.; Guichard, G. Anion recognition by aliphatic helical oligoureas. *Chem. Eur. J.* **2016**, *22*, 15684–15692. [[CrossRef](#)]
111. Pihko, P.M. Activation of carbonyl compounds by double hydrogen bonding: An emerging tool in asymmetric catalysis. *Angew. Chem. Int. Ed. Engl.* **2004**, *43*, 2062–2064. [[CrossRef](#)] [[PubMed](#)]
112. Doyle, A.G.; Jacobsen, E.N. Small-molecule H-bond donors in asymmetric catalysis. *Chem. Rev.* **2007**, *107*, 5713–5743. [[CrossRef](#)] [[PubMed](#)]
113. Fang, X.; Wang, C.J. Recent advances in asymmetric organocatalysis mediated by bifunctional amine-thioureas bearing multiple hydrogen-bonding donors. *Chem. Commun.* **2015**, *51*, 1185–1197. [[CrossRef](#)] [[PubMed](#)]
114. Maruoka, K. *Science of Synthesis: Asymmetric Organocatalysis Vol. 2: Brønsted Base and Acid Catalysts, and Additional Topics*; Thieme Publishing Group: Stuttgart, Germany, 2012.
115. Jones, C.R.; Dan Pantos, G.; Morrison, A.J.; Smith, M.D. Plagiarizing proteins: Enhancing efficiency in asymmetric hydrogen-bonding catalysis through positive cooperativity. *Angew. Chem. Int. Ed. Engl.* **2009**, *48*, 7391–7394. [[CrossRef](#)]

116. Probst, N.; Madarasz, A.; Valkonen, A.; Papai, I.; Rissanen, K.; Neuvonen, A.; Pihko, P.M. Cooperative assistance in bifunctional organocatalysis: Enantioselective Mannich reactions with aliphatic and aromatic imines. *Angew. Chem. Int. Ed. Engl.* **2012**, *51*, 8495–8499. [[CrossRef](#)]
117. Pengo, B.; Formaggio, F.; Crisma, M.; Toniolo, C.; Bonora, G.M.; Broxterman, Q.B.; Kamphuis, J.; Saviano, M.; Lacovino, R.; Rossi, F.; et al. Linear oligopeptides. Part 406.1 Helical screw sense of peptide molecules: The pentapeptide system (Aib)₄/L-Val[L-(α Me)Val] in solution. *J. Chem. Soc. Perkin Trans. 2* **1998**, 1651–1658. [[CrossRef](#)]
118. Brown, R.A.; Marcelli, T.; De Poli, M.; Sola, J.; Clayden, J. Induction of unexpected left-handed helicity by an N-terminal L-amino acid in an otherwise achiral peptide chain. *Angew. Chem. Int. Ed. Engl.* **2012**, *51*, 1395–1399. [[CrossRef](#)]
119. De Poli, M.; Byrne, L.; Brown, R.A.; Sola, J.; Castellanos, A.; Boddaert, T.; Wechsel, R.; Beadle, J.D.; Clayden, J. Engineering the structure of an N-terminal beta-turn to maximize screw-sense preference in achiral helical peptide chains. *J. Org. Chem.* **2014**, *79*, 4659–4675. [[CrossRef](#)]
120. Le Bailly, B.A.; Clayden, J. Controlling the sign and magnitude of screw-sense preference from the C-terminus of an achiral helical foldamer. *Chem. Commun.* **2014**, *50*, 7949–7952. [[CrossRef](#)]
121. Le Bailly, B.A.; Byrne, L.; Clayden, J. Refoldable foldamers: Global conformational switching by deletion or insertion of a single hydrogen bond. *Angew. Chem. Int. Ed. Engl.* **2016**, *55*, 2132–2136. [[CrossRef](#)]
122. David, R.; Gunther, R.; Baumann, L.; Luhmann, T.; Seebach, D.; Hofmann, H.J.; Beck-Sickinger, A.G. Artificial chemokines: Combining chemistry and molecular biology for the elucidation of interleukin-8 functionality. *J. Am. Chem. Soc.* **2008**, *130*, 15311–15317. [[CrossRef](#)] [[PubMed](#)]
123. Lee, B.C.; Zuckermann, R.N. Protein side-chain translocation mutagenesis via incorporation of peptoid residues. *ACS Chem. Biol.* **2011**, *6*, 1367–1374. [[CrossRef](#)] [[PubMed](#)]
124. Craven, T.W.; Bonneau, R.; Kirshenbaum, K. PPII helical peptidomimetics templated by cation- π interactions. *Chembiochem* **2016**, *17*, 1824–1828. [[CrossRef](#)]
125. Mayer, C.; Muller, M.M.; Gellman, S.H.; Hilvert, D. Building proficient enzymes with foldamer prostheses. *Angew. Chem. Int. Ed. Engl.* **2014**, *53*, 6978–6981. [[CrossRef](#)]
126. Hegedus, Z.; Grison, C.M.; Miles, J.A.; Rodriguez-Marin, S.; Warriner, S.L.; Webb, M.E.; Wilson, A.J. A catalytic protein-proteomimetic complex: Using aromatic oligoamide foldamers as activators of RNase S. *Chem. Sci.* **2019**, *10*, 3956–3962. [[CrossRef](#)]
127. Muller, M.M.; Kries, H.; Csuhai, E.; Kast, P.; Hilvert, D. Design, selection, and characterization of a split chorismate mutase. *Protein Sci.* **2010**, *19*, 1000–1010. [[CrossRef](#)] [[PubMed](#)]
128. Pervushin, K.; Vamvaca, K.; Vogeli, B.; Hilvert, D. Structure and dynamics of a molten globular enzyme. *Nat. Struct. Mol. Biol.* **2007**, *14*, 1202–1206. [[CrossRef](#)]

